Detection of Extreme Waves using Synthetic Aperture Radar Images

S. Lehner, J. Schulz-Stellenfleth,A.Niedermeier

German Aerospace Center (DLR), D-82234 Oberpfaffenhofen, Germany

Abstract— **Within the last years a considerable number of large ships have been lost due to severe sea state conditions. The cause of accidents are in many cases believed to be rogue waves, which are individual waves of exceptional wave height or abnormal shape. In particular steep breaking waves can be fatal for smaller ships. Damage is sometimes also be caused by unusual grouping of waves, which can lead to dangerous ship motion.**

In situ measurements of extreme waves are sparse with most observations reported by ship masters after the encounter. In this paper a global data set of 5 x 10 km sized synthetic aperture radar (SAR) images acquired by the European Remote Sensing satellite ERS-2 every 200 km along the track is used to analyse extreme ocean wave events. As the European Space Agency (ESA) does not provide this dataset as a standard product wave mode raw data were reprocessed to complex SAR images using the processor BSAR developed at the German Aerospace Center (DLR). About 1000 globally distributed SAR wave mode images are available every day.

Two dimensional ocean wave fields are derived from SAR images by inversion of the SAR imaging mechanism. Individual high waves are detected in the derived wave fields using a matched filter technique.

The inhomogeneity of ocean wave fields is analysed using a parameter, which describes the shift invariance of the wave spectrum.

I. Introduction

Traditionally ocean wave measurements with synthetic aperture radar (SAR) data are based on a spectral approach. Different schemes to derive ocean wave spectra from given SAR spectra have beeen proposed [1], [2], [3].

To take advantage of the full high resolution image information ERS-2 wave mode raw data were processed to single look complex SAR imagettes, that are not available as a standard ESA product, using the BSAR processor, developed at the German Space Agency (DLR). In total 34 310 SAR imagettes acquired every 200 km along the track were processed representing 27 days of data between August 21, 1996 and June 2, 1997. Studies on the use of ERS wave mode data for wind and wave measurements were published in [4], [5], [6] (this issue) and [7], [1], [8]. Wind direction can be retrieved from wind induced streaks and wind speed from the mean normalized radar cross section of the SAR imagette using the C-band model CMOD4, which was originally developed for the ERS scatterometer (SCAT).

Fig. 1 shows two imagettes from the reprocessed data set with ocean wave patterns. Details about the processing of wave mode data and a first comparison with ocean wave model data provided by the European Centre for Medium Range Weather Forecast (ECMWF) can be found in [5]. Having the full image information available the reprocessed data set allows to apply image analysis techniques for detection of individual waves and wave groups on a global scale.

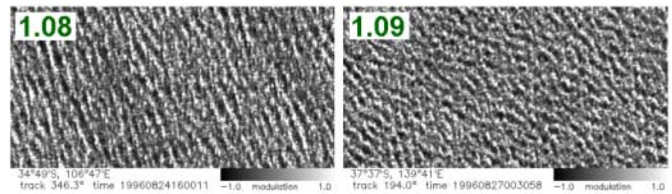

Fig. 1. Two ERS-2 imagettes of 10 by 5 km size reprocessed from wave mode raw data using the DLR BSAR processor. The resolution is about 20 m.

II. SAR retrieval of a sea surface elevation field

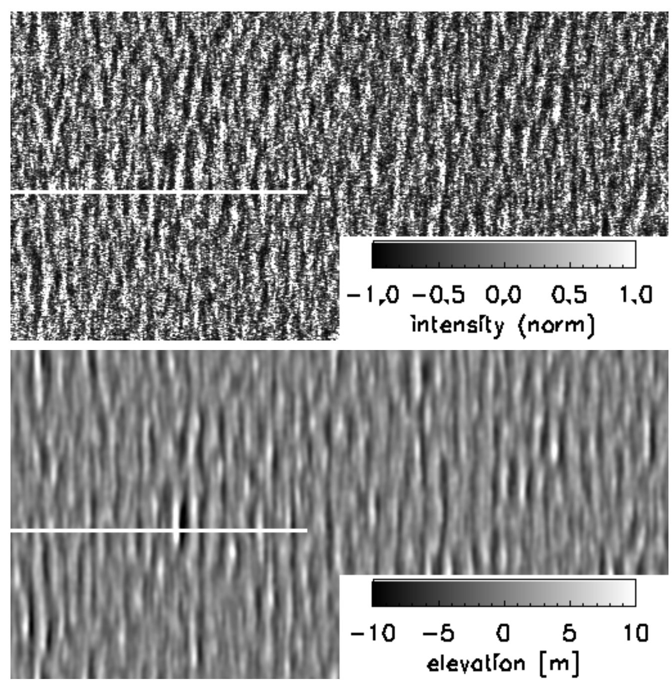

Fig. 2. SAR ocean wave retrieval in the spatial domain. The top image shows a normalized ERS-2 wave mode imagette acquired at 48.45°S, 10.33°E on Aug 27, 19969, 22:44 UTC. On the bottom the retrieved sea surface elevation field is shown.

Instead of doing the SAR ocean wave retrieval in the spectral domain ocean wave fields can be derived by inversion of the SAR image itself. Using a Fourier representation of the ocean wave field ζ

$$\zeta(x,t) = 2\; Re[\sum_k \zeta_k \exp(-i(k\,x - \omega\,t))] \qquad (1)$$

the corresponding normalised SAR intensity image at time $t = 0$ is given by

$$\frac{I(x) - \langle I \rangle}{\langle I \rangle} = 2\; Re[\sum_k \; \zeta_k \, T_k^S \; \exp(-i\,k\,x)] \qquad (2)$$

where we have used a quasilinear approximation. Here T^S is the SAR transfer function [9], ω is wave frequency, and ζ_k are the complex Fourier coefficients. Using the directional information contained in cross spectra [10] the mapping relation given by eq. 1 can be inverted. Note that this quasilinear inversion technique is in general only feasable in cases where the dominant wave system is travelling in the approximate across flight (range) direction, as too much spectral energy is lost due to the azimuthal cut-off mechanism [9] otherwise. Fig. 3 shows a retrieval of a sea surface elevation field (B) using a normalized ERS-2 SAR imagette (A). The image was acquired in the south Atlantic with about 10 m significant waveheight according to the ocean wave model run at the ECMWF. Application of the inversion scheme described in [11] (this issue) using the ECMWF spectrum as prior knowledge gave a slightly higher H_s of 11.5 m.

III. Detection of extreme individual waves

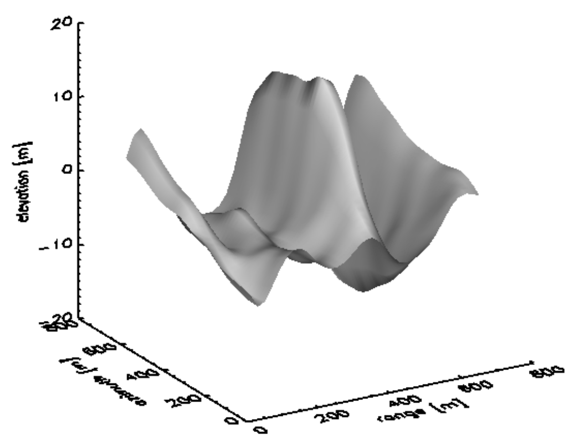

Fig. 3. Surface plot of an individual wave of about 30 m height found in ERS-2 SAR data.

The highest individual wave in the derived ocean wave field was detected by using a matched filter approach. The required model for an individual wave is based on a harmonic wave, which decays both in the propagation direction defined by the peak wavenumber vector $\mathbf{k_p}$ and in the across propagation direction.

$$m(\mathbf{x}) = \cos(\mathbf{k_p}\,\mathbf{x}) \; \exp(-\alpha(\mathbf{k_p^\perp}\;\mathbf{x})^2 - \beta(\mathbf{k_p}\,\mathbf{x})^2) \qquad (3)$$

Here $\mathbf{k_p}$ is the peak wavenumber vector found in the retrieved wave spectrum and α and β are parameters describing the rate of decay in k_p and $k_p^\perp$ direction. The box in Fig. 3 indicates the location of the highest individual wave found by searching for the maximum of the cross covariance function of ocean wave field and individual wave model eq. 3. Fig. 4 shows the respective cut through the wave field. It can be seen that the detected individual wave has a height of about 30 m. With a corresponding significant waveheight of 10 m this wave can be called a rogue wave according the requirement $\geq 2\,H_s$ which is often used as a definition.

SAR measurement of sea surface elevation fields instead of the corresponding spectra opens up a new field of ocean wave analysis techniques. With the restrictions mentioned above it is possible to investigate non-gaussian features of ocean waves, which can e.g. be caused by rogue waves.

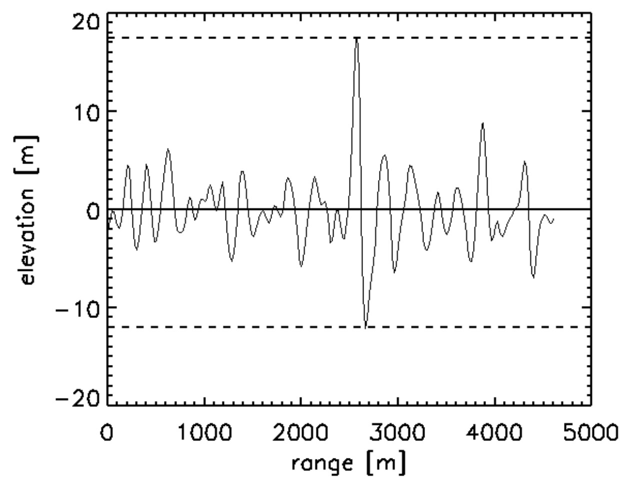

Fig. 4. Cut through the retrieved ocean wave field in range direction as indicated in Fig. 3.

IV. Global Maps of extreme wave height

Up to now only a limited test data set of about three weeks of imagette data in 1996 and 1997 is available. Usually data are stored only as rather coarsely gridded image spectra. This SAR data set was inverted to individual wave heights and investigated for individual wave height and steepness. The wave mode data images of the ENVISAT satellite will be available operationally, thus allowing a global overview of the ocean surface.

Fig. 5 shows the maximum wave height found for this data set on a three by three degree grid. Data are from the time period between August, 21st, 1996 to September, 8th, 1996, October, 4th, 1996 to October 9th, 1996 and a short time period of June first to second 1997. The highest individual waves are found in the area around Antarctica as expected. The highest individual wave event detected in this dataset happened on August 20th, 1996 at 22:51:17 UTC, 44.6 degrees south and 7.1 deg. east with a crest to trough waveheight of 29.8 m. For this case maximum to significant waveheight is then 2.9. Furthermore the storm track of the hurricane FRAN approaching Florida can be observed in the Atlantic between 20 and 30 degrees northern latitude. Individual waveheights between 15 and 18 m are observed. Due to the short fetch highest waves do not occur in hurricanes as expected. Of course these results have still to be treated with care as measurement of individual waveheights of radar images could not be validated up to now.

Figure 6 shows a global map on a 3 x 3 degree grid of the maximum steepness derived from the SAR derived digital elevation model of the sea surface. It can be seen that the steepness has a similar global distribution as the maximum wave height with the most extreme values observed in the south Atlantic.

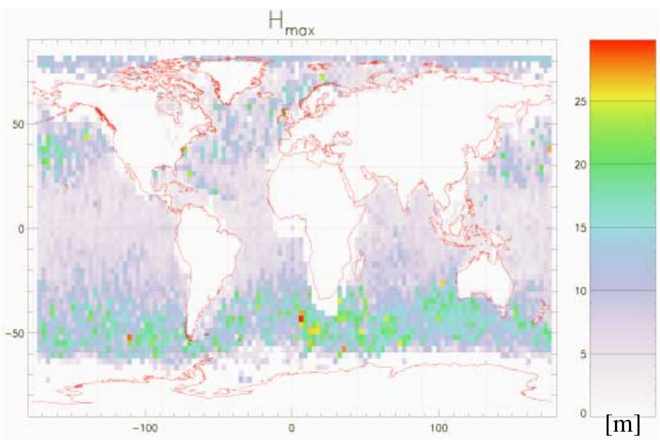

Fig. 5. Global map of heighest individual waves heights detected in a data set of ERS-2 imagettes acquired within three weeks.

V. Conclusions and Outlook

The remote sensing techniques described in this study help to find empirical relationships between mean sea state characteristics and probabilities of extreme wave events. Furthermore "hot spots" are identifiedand thus to improve risk maps of extreme individual wave events. Obviously this data set comprises too short a time frame to give validated long term statistics on extreme wave heights. It is therefore intended to reprocess the wave mode data set for the full lifetime of the ERS satellites and extend the study to the recent ENVISAT data. Validation of the proposed methods is planned using buoy and laser measurements as well as data acquired by ground-based radar [12] (this issue).

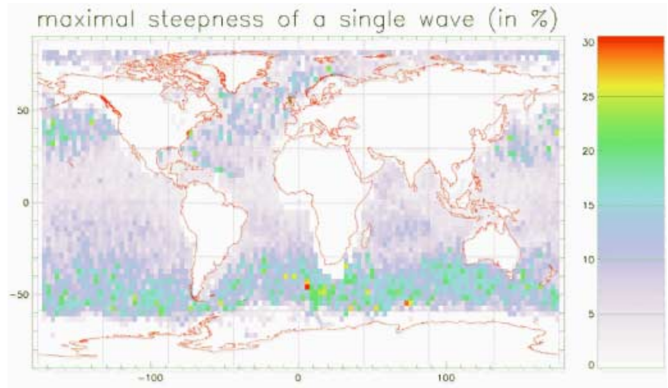

Fig. 6. Global map of maximum wave steepness detected in a data set of ERS-2 imagettes acquired within three weeks.

It is expected that the presented approach will give new insight into different aspects of ocean wave physics like, e.g. wave breaking.

References

[1] S. Hasselmann, C. Brüning, K. Hasselmann, and P. Heimbach, "An improved algorithm for the retrieval of ocean wave spectra from synthetic aperture radar image spectra," *J. Geophys. Res.*, vol. 101, pp. 16615–16629, 1996.

[2] H. Krogstad, O. Samset, and P. W. Vachon, "Generalizations of the nonlinear ocean-SAR transformation and a simplified SAR inversion algorithm," *Atmos. Ocean*, vol. 32, pp. 61–82, 1994.

[3] C. Mastenbroek and C. F. de Valk, "A semi-parametric algorithm to retrieve ocean wave spectra from synthetic aperture radar," *J. Geophys. Res.*, vol. 105, pp. 3497–3516, 2000.

[4] V. Kerbaol, B. Chapron, and P. W. Vachon, "Analysis of ERS-1/2 synthetic aperture radar wave mode imagettes," *J. Geophys. Res.*, vol. 103, pp. 7833–7846, 1998.

[5] S. Lehner, J. Schulz-Stellenfleth, B. Schättler, H. Breit, and J. Horstmann, "Wind and wave measurements using complex ERS-2 SAR wave mode data," *IEEE, TGARS*, vol. 38, pp. 2246–2257, 2000.

[6] Jochen Horstmann, Wolfgang Koch, and Susanne Lehner, "High resolution wind fields retrieved from SAR in comparison to numerical models," in *Proc. Int. Geosci. Remote Sens. Symp.*, Toronto, Canada, 2002.

[7] P. Heimbach, S. Hasselmann, and K. Hasselmann, "Statistical analysis and intercomparison with WAM model data of three years of global ERS-1 SAR wave mode spectral retrievals," *J. Geophys. Res.*, vol. 103, pp. 7931–7977, 1998.

[8] J. Schulz-Stellenfleth, S. Lehner, and D. Hoja, "Retrieval of ocean wave spectra from complex synthetic aperture radar data," in *Proceedings of the 4th Berlin Workshop on Ocean Remote Sensing*, 2001.

[9] K. Hasselmann and S. Hasselmann, "On the nonlinear mapping of an ocean wave spectrum into a synthetic aperture radar image spectrum," *J. Geophys. Res.*, vol. 96, pp. 10713–10729, 1991.

[10] G. Engen and H. Johnson, "SAR-ocean wave inversion using image cross spectra," *IEEE Trans. Geosci. Rem. Sens.*, vol. 33, pp. 1047–1056, 1995.

[11] J. Schulz-Stellenfleth, S. Lehner, and D. Hoja, "A parametric scheme for ocean wave retrieval from complex sar data using prior information," in *Proceedings of the IGARSS2002 conference, Toronto, Canada*, 2001.

[12] H. Dankert, J. Horstmann, and W. Rosenthal, "Detection of extreme ocean waves using radar-image sequences," in *Proc. Int. Geosci. Remote Sens. Symp. 1998*, Toronto, Canada, 2002.